Theory of solvation-controlled reactions in stimuli-responsive nanoreactors

Stefano Angioletti-Uberti,[1,2] Yan Lu,[2] Matthias Ballauff,[1,2] and Joachim Dzubiella[1,2,*]

[1] *Institut für Physik, Humboldt-Universität zu Berlin, Newtonstr. 15, Berlin, Germany*

[2] *Helmholtz-Zentrum Berlin, Hahn-Meitner-Platz 1, Berlin, Germany*

Abstract

Metallic nanoparticles embedded in stimuli-responsive polymers can be regarded as nanoreactors since their catalytic activity can be changed within wide limits: the physicochemical properties of the polymer network can be tuned and switched by external parameters, such as, e.g., the temperature or the pH, and thus allows a selective control of reactant mobility and concentration close to the reaction site. Based on a combination of Debye's model of diffusion through an energy landscape and a two-state model for the polymer, here we develop an analytical expression for the diffusional part k_D of the rate constant. The rate k_D has two factors that can switch upon the action of an external stimulus: i) the diffusivity of the reactants in the network that enters linearly into k_D, and ii) the solvation free enthalpy change $\Delta\bar{G}_{\rm sol}$ for network permeation that enters exponentially. Thus, $\Delta\bar{G}_{\rm sol}$ which describes the partitioning of the reactant in the network versus bulk is the decisive term in most cases. A comparison with recent experimental data on switchable, thermosensitive yolk-shell nanoreactors demonstrates the general validity of the concept.

I. INTRODUCTION

Metallic and oxidic nanoparticles have been the subject of intense studies in recent decades because of their catalytic activity.[1,2] For example, gold becomes an active catalyst for oxidation reactions when divided down to the nanoscale.[3–5] Titania nanoparticles are also highly active catalysts[6,7] and there is a large number of other nanometric systems with promising catalytic properties.[1] Use in catalytic reaction requires a simple and secure handling of nanoparticles by a suitable macromolecular carrier system, in particular when working in solution. Such a carrier system should not impede the catalytic activity of the nanoparticles but keep them firmly stabilized throughout the reaction and the subsequent work-up. Reactants should be able to enter and leave the carrier without major diffusional resistance. A catalytic system thus defined acts in many ways as a nanoreactor, that is, it contains and shelters the catalytic reaction. Examples of these nanoreactors are given, e.g., by dendrimeric systems[8] or those based on spherical polyelectrolyte brushes.[9]

In recent years, a new class of carrier systems is emerging that can be termed active nanoreactors.[10–17] Here the nanoparticles are embedded in a polymer gel that reacts to external stimuli. In the liquid phase the diffusional resistance may be manipulated by parameters such as temperature or pH. The best-studied examples of such active carriers are colloidal gels made from crosslinked poly(N-isopropylacrylamide) (PNIPAM) that undergo a volume phase transition at 32^{o}C. Thus, it has been demonstrated that the catalytic activity of metal nanoparticles embedded in a PNIPAM gel can be manipulated using temperature as the external stimulus.[10]

In particular, a simple model system has been prepared by enclosing a single gold nanoparticles in a hollow PNIPAM sphere, a so-called yolk-shell architecture.[15] This active carrier in aqueous phase provides the ideal means to investigate the manipulation of the activity of a nanoparticle in a stimuli-responsive nanoreactor. It has been demonstrated that the reactivity of the nanoparticle can be switched depending on the hydrophilicity of the reactants.[15] These findings open a new way to introduce selectivity into the catalysis with nanoparticles. Another model system introduced by the Vigo group is made up by a single gold particle embedded in the middle of a colloidal PNIPAM sphere, a core-shell architecture. Here Carregal-Romero *et al.* demonstrated that the reduction of hexacyanoferrate (III) ions by sodium borohydride is slowed down drastically above the temperature of the volume transi-

tion, that is, when the gel has shrunken and most of the water has been expelled.[13] These workers explained this decrease of the kinetic constant by the decrease in the reactant's diffusion (or mobility) in the gel in its dense, shrunken state using a two-state model for the gel. In this way Carregal-Romero *et al.* presented the first theory of the kinetics of catalysis by nanoparticles in such an active nanoreactor.

Studying the reactivity of nanoparticles in the condensed phase requires a model reaction that allows us to obtain kinetic parameters related to catalysis with greatest possible precision. Based on the pioneering work of Pal *et al.*[18] and Esumi *et al.*,[19] we[20–25] and many others[17,26–34] have demonstrated that the reduction of nitroarenes and especially of nitrophenol by borohydride ions in aqueous phase fulfills all the requirements for such a model reaction:[34] The concentration of the reactant 4-nitrophenol can be monitored easily and with high precision by UV/VIS-spectroscopy and there is only one final product, namely 4-aminophenol. Thus, this reaction proceeds virtually without side reactions. A recent study has developed a detailed kinetic model that includes 4-hydroxylaminophenol as the most stable intermediate.[25] Using this model reaction, Wu *et al.* were able to show that the reactivity of the rather hydrophobic nitrobenzol is even increased when raising the temperature above the temperature of the volume transition.[15] This finding cannot be rationalized anymore in terms of a changed diffusivity of the reactants. Wu *et al.* called attention on the fact that the thermodynamic interaction of the reactants with the PNIPAM network must be considered as well. Using Debye-Smoluchowski theory of diffusion on an energy landscape,[35,36] Wu *et al.* demonstrated that the diffusion constant enters linearly in the expression of the kinetic constant whereas the thermodynamic interaction as expressed through the respective free enthalpy ΔG_{solv} of the reactant in the network enters exponentially. Hence, the reactivity is ultimately governed by ΔG_{solv}.[15]

Here we present the full theory of nanoreactors that combines our previous analysis[15] with a two-state model[13,37,38] that takes into account the thermodynamic transition within the gel. The predictions of this model are compared to recent experimental data for the particular architecture of yolk-shell systems[15] which includes core-shell as a special limit. The remainder of the paper is organized as follows: in Sec. II, we present our theory. In section III we discuss its results in light of available experimental data and state a few of its consequences for the design of nanoreactors. A brief Conclusion will wrap up all results together with suggestion for further research.

II. THEORY

A. Kinetics of surface reactions

We start with the rate equation describing a chemical reaction of first order:

$$\frac{dc_0(t)}{dt} = -k_{\rm exp} c_0(t) \tag{1}$$

where c_0 is the concentration of reactants in solution, and $k_{\rm exp}$ is the experimental rate constant. By using a microscopic description we will arrive at an expression for the number of reactants transformed by the nanoreactor per unit time *at a constant bulk density* c_0, ending up with an equation of the form:

$$\frac{dN}{dt} = k_{\rm obs} c_0. \tag{2}$$

In order to connect $k_{\rm exp}$ and $k_{\rm obs}$, one needs to make two assumptions: The first is that, if we work at low enough concentrations of nanoreactors (which is always the case under relevant experimental settings), these will not interact and can be treated independently (i.e., we can use a cell model, as explained in more details elsewhere[39]). Furthermore, we assume that although the bulk concentration c_0 changes in time, it does so slow enough that the steady state solution Eq. (2) is always a good approximation. Experimentally, we look into the initial rates of reaction. Thus,

$$\begin{aligned} \frac{dN}{dt} &= -k_{\rm obs} c_0 \\ \frac{1}{V_{\rm sol}} N_{\rm nano} \frac{dN}{dt} &= -\frac{1}{V_{\rm sol}} N_{\rm nano} k_{\rm obs} c_0 \\ \frac{dc_0}{dt} &= -\frac{1}{V_{\rm sol}} N_{\rm nano} k_{\rm obs} c_0 \end{aligned} \tag{3}$$

leading to

$$k_{\rm exp} = -\frac{1}{V_{\rm sol}} N_{\rm nano} k_{\rm obs} \tag{4}$$

where $N_{\rm nano}$ is the total number of nanoreactors present in a volume $V_{\rm sol}$ of solution. Eq. (4) provides a link from the rate $k_{\rm exp}$ typically used to describe experiments and the microscopic rate at which nanoreactors transform reactants.

We also notice that often in the literature the reaction rate per total surface area of catalyst (i.e., total nanoparticle surface area) per volume of solution is reported[20,22–25,34]

$$\tilde{k}_{\mathrm{exp}} = \frac{k_{\mathrm{exp}}}{S_{\mathrm{tot}}/V_{\mathrm{sol}}} = \frac{N_{\mathrm{nano}} k_t}{S_{\mathrm{tot}}} = \frac{k_{\mathrm{t}}}{S_0} \tag{5}$$

where S_0 is now the surface area of a single nanoparticle inside the nanoreactor. Via Eq. (5), we see how this latter normalized constant $\tilde{k}_{\mathrm{exp}}$ is truly an intensive measure of the properties of a single-nanoreactor, and is the quantity that should be used for comparison within different systems. We next proceed to describe our microscopic model for the calculations of k_{t}.

B. Model

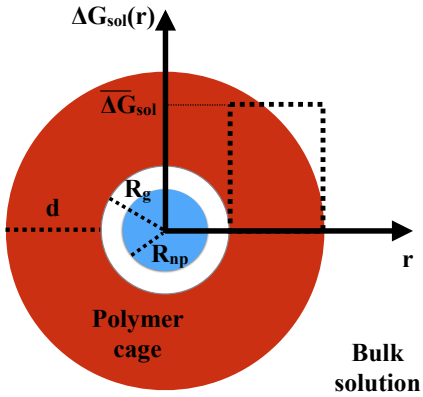

FIG. 1: Schematic representation of a yolk-shell nanoreactor and central quantities for our theory. At the centre core of the nanoreactor sits a metal nanoparticle (blue) of radius R_{np}, embedded in a spherical polymer shell ('cage') of inner radius R_g and outer radius $R_g + d$. The reactants have to overcome a solvation free enthalpy barrier $\Delta G_{\mathrm{sol}}(r)$ to reach the nanoparticle depicted by the dotted lines. In our model, $\Delta G_{\mathrm{sol}}(r)$ is represented as a piecewise constant function, of value $\Delta \bar{G}_{\mathrm{sol}}$ inside the polymer shell, and zero otherwise. In the case shown, $\Delta \bar{G}_{\mathrm{sol}}$ is higher in the gel than in the bulk solution, representing "polymer-phobic" reactants, with an energetic penalty to absorb inside the shell, but the opposite situation can also occur.

A schematic representation of a yolk-shell nanoreactor is shown in Fig. 1. For such a spherically symmetric system, we intend to model the rate for the catalytic reaction occurring at the surface of the nanoparticle, which requires taking into account the diffusion process that brings a reactant from the bulk solvent to the surface of the nanoparticle inside the nanoreactor's core.[15] The kinetics of this process is governed by two key functions, the mobility of the reactants along the trajectory expressed by a diffusivity profile $D(r)$ and a thermodynamic free energy of solvation profile $\Delta G_{\mathrm{sol}}(r)$. This local free enthalpy $\Delta G_{\mathrm{sol}}(r)$ measures the difference in the local excess chemical potential and the 'reservoir' chemical potential of the reactants far away from the nanoreactor. Along its trajectory, the reactant encounters a different chemical environment in the gel, and its average interaction with it then results in local $D(r)$ and $\Delta G_{\mathrm{sol}}(r)$ different than in bulk.

In order to keep the model as simple as possible, we take both $D(r)$ and $\Delta G_{\mathrm{sol}}(r)$ to be a step function centered in the polymer cage of the nanoreactor, of width equal to the shell width d (see Fig. 1 for reference). This is a good approximation for spatially homogeneous gels that have been under consideration recently.[15] Thus, we get:

$$D(r) = \begin{cases} D_0 & \text{for } r < R_{\mathrm{g}} \text{ or } r > R_{\mathrm{g}} + d \\ D_{\mathrm{g}} & \text{for } R_{\mathrm{g}} \leq r \leq R_{\mathrm{g}} + d \end{cases} \tag{6}$$

and

$$\Delta G_{\mathrm{sol}}(r) = \begin{cases} 0 & \text{for } r < R_{\mathrm{g}} \text{ or } r > R_{\mathrm{g}} + d \\ \Delta \bar{G}_{\mathrm{sol}} & \text{for } R_{\mathrm{g}} \leq r \leq R_{\mathrm{g}} + d \end{cases} \tag{7}$$

where R_{g} is the inner radius of the polymer shell and d its width, cf. Fig.1. The choice of step functions basically implies that a reactant sees only two distinct environments, the interior of the polymer shell or the bulk solution. Hence, in this form, $\Delta \bar{G}_{\mathrm{sol}}$ can be identified with the difference in the solvation free enthalpy of the reactants in the gel with respect to that in the bulk solvent. As such, $\Delta \bar{G}_{\mathrm{sol}}$ does not depend solely on the reactant-polymer interaction, but also on the solvent constituting the bulk solution. By measuring the equilibrium partitioning coefficient of the molecule in the gel K_{eq}, $\Delta \bar{G}_{\mathrm{sol}}$ can be measured experimentally, or computed via atomistic simulations, with the following equation:

$$K_{\mathrm{eq}} = c_g / c_0 = \exp[-\beta \Delta \bar{G}_{\mathrm{sol}}] \tag{8}$$

where c_g and c_0 are the equilibrium concentrations of reactant in the polymer gel and in

the bulk solution, respectively, and $\beta = 1/k_{\mathrm{B}}T$ is the thermal energy.

C. Diffusion in hydrogels: Modeling of D_{g}

The diffusion of solutes through hydrogels is a complex process[40,41] and depends not only on the individual properties of the polymer, solvent, and solutes, such as size and concentration, but also on the particular interactions of the solute with the polymer network. In our case we restrict the discussion to the case of homogenenous gels with semiflexible polymers in the dilute and semi-dilute regimes with very small diffusing solutes with a size comparable to a polymer monomer. Since for the latter system relatively weak and slippery hydrophobic attractions ($\beta\epsilon \simeq 1$) are assumed to be at work we can conclude that the diffusion process is mainly governed by a combination of translating around the the obstructing polymer chains and partial sliding along the chains. In this case obstruction or hydrodynamic theories for small diffusing particles should be applicable.[40,41] We employ the relatively general form

$$D_{\mathrm{g}} = D_0 \exp(-a\phi^{\nu}), \tag{9}$$

where D_{g} and D_0 are the gel and bulk diffusion coefficient, respectively, whereas a and ν are system dependent parameters. The coefficient a is often related to the ratio of solute size and polymer size with prefactors on the order of unity.[40,41] Since we operate in the small solute limit we will set $a = 1$. The exponent ν can vary between 0.5 and 1 dependent on the theoretical assumptions. We will use $\nu = 0.75$, the proper value based on scaling concepts for flexible chains in homogeneous gels.[40,41]

We emphasize that all theoretical approaches to the diffusion process in our regimes predict a decrease of diffusion for higher packing fractions. The detailed form of Eq. (9) is thus not of importance to discuss the qualitative features of the temperature dependence of the reaction rate of nanoreactors. The latter is expressed in Eq. (9) by the temperature dependence of the packing fraction $\phi(T)$. While one also could suspect effects of the T-dependence of the intrinsic binding constant $\epsilon(T)$ on the diffusion process, we believe that these effects are of higher order in our operating regime, where we assume only a weak attraction of solutes to the polymer chain $\beta\epsilon \lesssim 1$. This could change for large attractions $-\beta\epsilon \gg 1$ where Arrhenius like activation terms have to enter into Eq. (9), as described in

the reviews.[40,41]

D. Coupling spatial diffusion and reaction: Debye-Smoluchowski approach

Once the diffusivity profile and the underlying free enthalpy on which the diffusing reactant must move to reach the surface of the nanoparticle are specified, it is possible to use an approach, initially developed by Smoluchowski[36] and then extended by Debye[35], to calculate the diffusion-controlled part of the reaction rate in our system. This approach was first used to describe the rate of collision between charged ions in solution,[35] but the underlying physical picture is equivalent to our model. For the reader's convenience we provide a step-by-step derivation of the final equations in the Appendix V, and we also suggest to consult the reviews of Calef and Deutch[42] and Berg and von Hippel[43] on diffusion-controlled reactions. The Debye-Smoluchowski model describes the rate at which a particle, driven by gradients in the chemical potential, diffuse from a bulk solution kept at constant concentration c_0 towards a fixed sink of radius R_{np}. Close to the sink, a reactive fraction per unit time of the molecules arriving are allowed to absorb ('react') as expressed by a surface reaction rate constant k_R. Restated in our language, the sink is nothing but the nanoparticle inside the nanoreactor, and absorption into the sink means reacting in the proximity of the nanoparticle's surface. The total reaction rate k_t, in units of reacting particles per unit time, arising from this model can be written as:

$$\begin{aligned} k_t^{-1} &= k_r^{-1} + k_D^{-1} \quad \text{or} \\ \tau_t &= \tau_r + \tau_D \end{aligned} \tag{10}$$

where the times τ_i defined in Eq. (10) are just the reciprocal of the respective rates, and should be interpreted as the effective time to diffuse to the sink τ_D, and to react once in the surface proximity in τ_r. Under these conditions the relation between the diffusivity and (free-)energy landscapes $D(r)$ and $\Delta G_{sol}(r)$, respectively, and the diffusion rate k_D is given

by the Smoluchowski/Debye expression (see the appendix)

$$k_D = 4\pi c_0 \left[\int_{R_{\rm np}}^{\infty} \frac{\exp\left[\beta \Delta G_{\rm sol}\left(r\right)\right]}{D(r) r^2} {\rm d}r \right]^{-1} . \tag{11}$$

E. Solving Debye's equation for yolk-shell nanoreactors

In k_D, an integral of $\Delta G_{\rm sol}\left(r\right)$ over space appears, which can be analytically expressed using our simplified step-wise forms for $D(r)$ and $\Delta G_{\rm sol}\left(r\right)$ valid for nanoreactors, see Eq. (7), obtaining:

$$\begin{aligned} k_D^{-1} &= \tau_D \qquad (12) \\ &= \int_{R_{\rm np}}^{\infty} \frac{\exp[\beta \Delta G(r)]}{4\pi r^2 c_0 D(r)} = \\ &= \int_{R_{\rm np}}^{R_{\rm g}} \frac{1}{4\pi r^2 c_0 D_0} + \int_{R_{\rm g}}^{R_{\rm g}+d} \frac{\exp[\beta \Delta \bar{G}_{sol}]}{4\pi r^2 c_0 D_{\rm g}} + \\ &\quad \int_{R_{\rm g}+d}^{\infty} \frac{1}{4\pi r^2 c_0 D_0} \\ &= \tau_{\rm np} + \tau_g + \tau_\infty \qquad (13) \end{aligned}$$

where again we split the typical time τ_D into three different contributions: the effective time to arrive from the bulk solution to the gel, τ_∞, that to cross the gel τ_g, and that to get to the surface of the nanoparticle once the gel has been crossed, $\tau_{\rm np}$.

Solving for the integrals in Eq. (13) gives the following result:

$$\begin{aligned} \tau_{\rm np} &= \frac{1}{c_0 4\pi D_0} \frac{R_{\rm g} - R_{\rm np}}{R_{\rm g}\, R_{\rm np}} \\ \tau_g &= \frac{\exp(\beta \Delta \bar{G}_{sol})}{c_0 4\pi D_{\rm g}} \frac{d}{(R_{\rm g}+d) R_{\rm g}} \\ \tau_\infty &= \frac{1}{c_0 4\pi D_0 (R_{\rm g}+d)} \end{aligned} \tag{14}$$

For typical nanoreactors, $d \gg R_{\rm g} \approx R_{\rm np}$ (which is exact when the reactor has a core-shell instead of a yolk-shell structure[15]). Considering also that $D_0 > D_{\rm g}$, one can further simplify Eq. 14 as:

$$\tau_{\mathrm{np}} \approx 0 \tag{15}$$

$$\tau_g \approx \frac{\exp(\beta \Delta \bar{G}_{sol})}{c_0 4\pi D_{\mathrm{g}} R_{\mathrm{g}}} \gg \tau_\infty, \tag{16}$$

Since the largest typical time, i.e. the slowest rate, dictates the final effective value for the reaction rate, the latter inequality implies:

$$\begin{aligned} k_D \approx 1/\tau_g &= 4\pi D_{\mathrm{g}} c_0 R_{\mathrm{g}} \ \exp\left(-\beta \Delta \bar{G}_{sol}\right) \\ &= 4\pi c_0 R_{\mathrm{g}} \ \mathcal{P} \end{aligned} \tag{17}$$

where we introduced the quantity $\mathcal{P} = D_{\mathrm{g}} \exp\left(-\beta \Delta \bar{G}_{sol}\right)$, sometimes referred to as "permeability" (or inverse diffusive resistance),[44,45] which takes into account the compounded effect of the diffusion coefficient and the solvation free enthalpy.
The dependence of the surface reaction rate k_r on temperature can be simply modelled using an Arrhenius equation:

$$k_r = k_r^0 \exp\left(-\beta \Delta E_r\right), \tag{18}$$

where ΔE_r is the activation energy of the surface reaction and k_r^0 is the reaction rate at zero barrier (see the discussion of this point in ref.[34]).

F. Coupling the Debye-Smoluchowski approach with a two-state-model

The stimuli-responsive polymer gels used as nanoreactors exhibit a volume transition between a swollen and a shrunken state at its lower critical solution temperature (LCST), T_{LCST} . The transition can be controlled by pH or other external control parameters and can be described using a two-state model.[13,37,38] Calling $\Delta G_{AB}\ (\xi) = \Delta G^A\ (\xi) - \Delta G^B\ (\xi)$ the difference of free enthalpy between these two states A and B, the Boltzmann-weighted probability to be in state A is given by:

$$p_{\mathrm{A}}(\xi) = \frac{\exp[-\beta \Delta G_{AB}\ (\xi)]}{1 + \exp[-\beta \Delta G_{AB}\ (\xi)]}. \tag{19}$$

where the quantity ξ is the external control parameter. In a two-state model, the probability of the system being in the B state is thus $1-p_{\mathrm{A}}(\xi)$. If one now assumes that a molecule coming from the bulk solution towards the gel will see one of the two environments with a probability given by Eq. (19), we arrive at the following equation for the total observed reaction rate:

$$k_{\mathrm{obs}} = \langle k_{\mathrm{t}} \rangle = p_{\mathrm{A}} k_{\mathrm{t}}^{A} + (1 - p_{\mathrm{A}}) k_{\mathrm{t}}^{B}. \tag{20}$$

where $(k_{\mathrm{t}}^{\alpha})^{-1} = k_{\mathrm{R}}^{-1} + k_{\mathrm{D}}^{-1}(\Delta \bar{G}_{\mathrm{sol},\alpha}, D_{\mathrm{g},\alpha})$, with $\alpha = A, B$. Eq. (20) is equivalent to considering a situation where a reactant diffuses in a constant environment. Each environment will give rise to a different rate, and the observed one is just the thermodynamic average between the two. This assumption, also implicitly made by Carregal-Romero *et al.* in their model,[13] becomes better the larger is the time it takes a system to swap between these two states of the gel compared with the average time a single reactant molecule takes to diffuse through the gel (which is of order d^2/D_{g}, and should not be confused by τ_{D}).

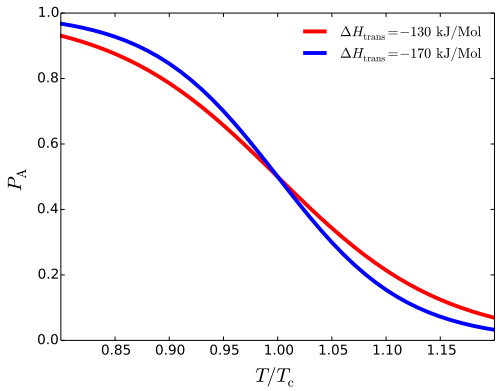

FIG. 2: Probability to find the system in the A state, $P_{\mathrm{A}}(\xi)$ as a function of the control parameter ξ in a thermodynamic two-states model, for two different values of the transition enthalpy ΔH_{AB}. The latter is defined through its connection with the transition free enthalpy via the standard relation $\Delta G_{AB}\ (\xi) = \Delta H_{AB} - T\Delta S_{AB}$. At the critical value for the control parameter ξ, p_{A} moves from 0 to 1, with increasing sharpness for increasing ΔH_{AB} (note that p_{B} is simply $1 - p_{\mathrm{A}}$).

On the opposite limit instead, when the gel switches infinitely fast between the two states, a reactant crossing the gel would see an average environment, i.e., an average solvation free

enthalpy and an average diffusion coefficient.[46] In this case, we have the following equation for the predicted rate:

$$k^{\text{fast}} = k_{\text{t}}(\langle \Delta \bar{G}_{\text{sol}} \rangle, \langle D_{\text{g}} \rangle), \tag{21}$$

where the two-state average $\langle .. \rangle$ of a quantity X is simply defined via the mean

$$\langle X \rangle = p_{\text{A}}(T) X_{\text{A}} + (1 - p_{\text{A}}(T)) X_{\text{B}}. \tag{22}$$

There is a quantitative difference in the reaction rates calculated within these two different

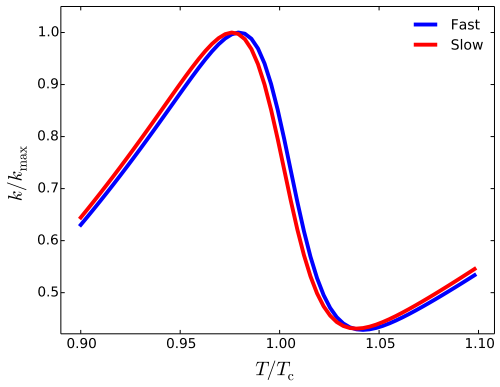

FIG. 3: Comparison of the reaction rate of a single nanoreactor calculated in the limit of infinitely fast (blue) and infinitely slow (red) swelling of the polymeric gel, i.e. using Eq. (22) and Eq. (20), respectively. The two limits describe qualitatively similar results, with only an apparent shift in the nanoreactor's behaviour as a function of the reduced temperature.

limits, as shown in Fig. 3, but both show the same qualitative trends. **what specific numbers are shown here, how general?**

We note, however, that in those cases where the swapping rate and the crossing rate are comparable, resonance effects might give an additional signature close to the transition temperature (cf., a review on stochastic resonance[47]). The investigation of those effects is out of scope of this paper and will be addressed in future studies.

Let us now describe the reaction rate behaviour resulting from Eq. (20): close to the critical value for the parameter ξ, i.e., where $\Delta G_{AB}\ (\xi) = 0$, the system continuously but sharply changes from the A to the B state (see Fig. 2). These two states of the polymer cage represent different physicochemical environments, hence we expect the solvation free

enthalpy $\Delta\bar{G}_{\rm sol}$ for a reactant to also change markedly between them. Since $\Delta\bar{G}_{\rm sol}$ enters exponentially in the observed reaction rate (Eq. 17), a sudden change upon polymer transition of $\Delta\bar{G}_{\rm sol}$ will be reflected by a concurrent sudden jump in $k_{\rm obs}$. However, given that also the diffusion coefficient will jump from two distinct values, the overall sign of the change will depend on the permeability $\mathcal{P}$ and not simply $\Delta\bar{G}_{\rm sol}$. Despite this, we notice that this latter quantity enters $\mathcal{P}$ explicitly exponentially, whereas the diffusion coefficient only linearly, and it is thus expected to play a larger role.

Eq. (20), together with the definitions in Eqs. (13) and (14), allows us to clarify the connection between our model and the model presented by Carregal-Romero *et al.*[13] If we set $\Delta\bar{G}_{\rm sol} = 0$, that is, had we not accounted for the interaction between polymer and reactant, Eq. (20) would be exactly equivalent to their model, which describes the reaction rate purely in terms of diffusion.

Eq. (17) further suggests another insightful way to interpret our results. The diffusion rate $k_{\rm D}$ in both models can be written as $k_{\rm D} = 4\pi RDc(R_{\rm g})$, where $c(R_{\rm g})$ is the local concentration of the reactant in the gel. In the model by Carregal-Romero *et al.* , $c(R_{\rm g}) = c_0$, i.e. the bulk concentration. In our model, since we consistently account for the thermodynamics of the system, we obtain $c(R_{\rm g}) = c_0 \exp[-\beta\Delta\bar{G}_{\rm sol}\,]$.

III. DISCUSSION

In the following, we shortly present a parametric study to demonstrate the influence of the various parameters in our model. For ease of discussion, and to make contact with a known and well studied system, that is PNIPAM-based yolk-shell nanoreactors, we take the external parameter ξ through which ΔG_{AB} is tuned to be temperature. Thus, the two two states of the gel are the low temperature swollen state A and the high temperature collapsed state B, and the variation in temperature of $\Delta\bar{G}_{\rm sol}$ is described via $\Delta\bar{G}_{\rm sol}\,,_\alpha = \Delta H_\alpha - T\Delta S_\alpha$ ($\alpha = A, B$), with $\Delta H_\alpha, \Delta S_\alpha$ being constants.

In order to highlight interesting trends dependent on $\Delta\bar{G}_{\rm sol}$, we take the case where the reaction rate is dominated by diffusion, i.e., $k_{\rm t} \approx k_{\rm D} << k_{\rm R}$. In the opposite case, the reaction rate would just follow the typical Arrhenius dependence dictated by Eq. (18), and the presence of the gel would not influence the reaction kinetics. Under the previous assumptions, Fig. 4 shows $k_{\rm obs}$ vs temperature (normalized by the transition temperature)

for three different scenarios. Panel A) shows k_{obs}, normalized by its maximum value within the plotted temperature interval $k_{\max}$, for changing $\Delta\Delta\bar{G}_{\mathrm{sol}} = \Delta G^{A}_{\mathrm{sol}} - \Delta G^{B}_{\mathrm{sol}}$ (i.e. the difference in solvation free enthalpy between the A and B state). When $\Delta\Delta\bar{G}_{\mathrm{sol}} > 0$, both terms appearing in $\mathcal{P}$ contribute to a drop in the rate, but it should be noticed that this drop is much stronger than it would be observed based on the drop in the diffusion coefficient alone. Indeed, this fact can explain the large drop of the "effective" diffusion coefficient necessary to fit rate-vs-temperature curves in the model of Carregal-Romero *et al.*[13], which is not compatible with Eq. (9). When $\Delta\Delta\bar{G}_{\mathrm{sol}} < 0$, k_{D} will depend on two contrasting effects: a decrease in the diffusion coefficient and an increase in the local concentration of reactant due to better solvation in the gel. In this case, for negative enough $\Delta\Delta\bar{G}_{\mathrm{sol}}$, a jump to higher rates is observed close to the transition temperature.

Whereas $\Delta\Delta\bar{G}_{\mathrm{sol}}$ dictates whether a jump or a drop in the rate occurs at the critical temperature, the absolute value of k_{obs} depends on the absolute value of $\Delta\bar{G}_{\mathrm{sol}}$. In Panel B, we fix $\Delta\Delta\bar{G}_{\mathrm{sol}}$ (< 0) by simply imposing $\Delta H = \Delta H_{\mathrm{B}} - \Delta H_{\mathrm{A}} = 5$ kJ/mol and varying the absolute value of ΔH_{B} (note that we do not normalize k_{obs} here). An important fact emerges. Whenever the solvation free enthalpy is positive the drop of the rate is proportional to $\exp(\Delta\Delta\bar{G}_{\mathrm{sol}})$ (and is hence equal for all curves) because Eq. (17) is basically exact, and the rate is dominated by crossing of the polymer gel ($\tau_{\mathrm{g}} \gg \tau_{\infty} \gg \tau_{\mathrm{np}}$). However, when the solvation free enthalpy becomes negative τ_{g} can decrease enough to be comparable or even below τ_{∞}. In this case, the rate is not proportional to $\exp(\Delta\Delta\bar{G}_{\mathrm{sol}})$ anymore and since τ_{∞} has a weaker dependence on temperature than τ_{g}, k_{obs} becomes almost constant. This becomes evident for the curve where $\Delta H_{\mathrm{B}} = -5$ kJ/mol, where the drop in the rate is just around 25% compared to an almost 20-fold decrease for the other cases. Finally, panel C) refers to the case where we can control the drop in the diffusion coefficient while keeping constant the solvation free enthalpy. In this case, we imposed the same $\Delta H_{A(B)}$ and $\Delta S_{A(B)}$ for all curves (giving $\Delta\Delta\bar{G}_{\mathrm{sol}} = -5$ kJ/mol), and we only change the diffusion coefficient in the B state. A situation similar to that observed in panel A) is seen: The chosen change in $\Delta\bar{G}_{\mathrm{sol}}$ would force an upward jump of the rate at the critical temperature, but this is counterbalanced by the drop expected due to a lower diffusion coefficient in the high-temperature, collapsed state. Depending on the relative magnitude of these two effects, i.e. on $\Delta\mathcal{P}$, different signatures are observed.

One last thing to notice in Fig. 4 is the behaviour of the rate as a function of temperature

away from the transition region. Whenever this is dictated by τ_{g} (i.e. when Eq. 17 is valid), the rate increases or decreases with temperature depending on the sign of the solvation enthalpy: a negative enthalpy means a decrease with temperature, whereas the opposite is observed for positive values, with the rate of decrease (i.e. the slope of the curve) being higher the higher the absolute value of ΔH.

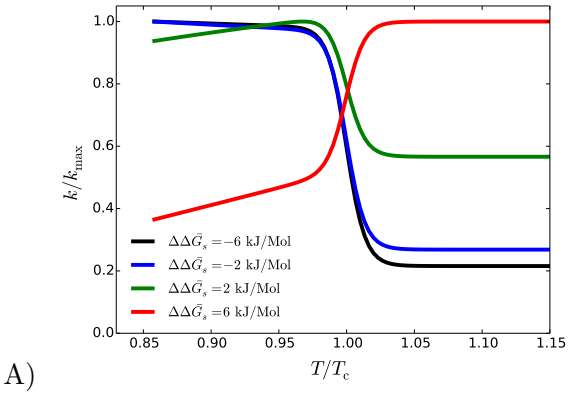

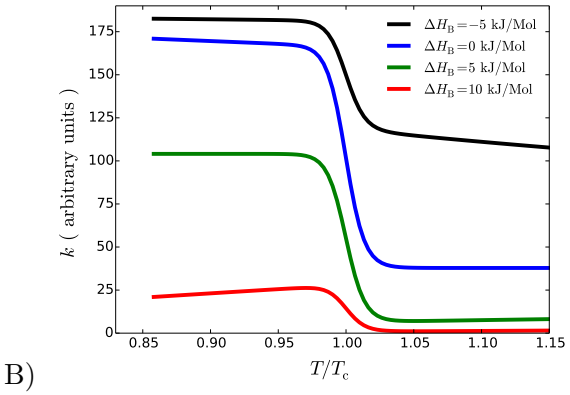

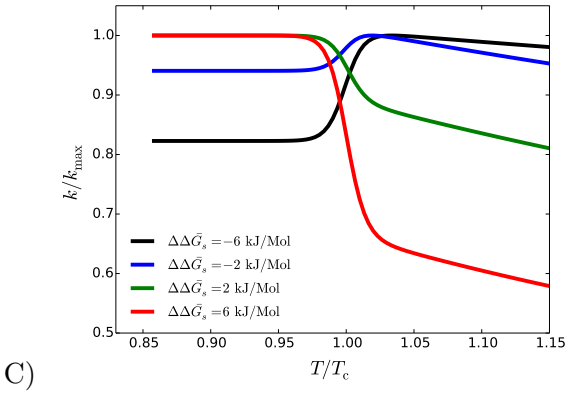

FIG. 4: Parameteric study of the influence of various factors on the reaction rate of nanoreactors as a function of temperature. A) For different $\Delta\Delta\bar{G}_{\mathrm{sol}} = \Delta G^B_{\mathrm{sol}} - \Delta G^A_{\mathrm{sol}}$ (and fixed value for $\Delta G^B_{\mathrm{sol}}$. B) At constant $\Delta\Delta\bar{G}_{\mathrm{sol}}$ (< 0), but changing the final value of $\Delta G^B_{\mathrm{sol}}$ via its enthalpy ΔH_{B}. C) For varying $\Delta = D_{\mathrm{B}}/D_{\mathrm{A}}$, i.e. for different drops in the diffusion coefficient in the collapsed state, in the case where $\Delta\Delta\bar{G}_{\mathrm{sol}}$ is constant (and < 0). This latter case shows how a large drop in diffusion coefficient can mask the effect of a decreasing free enthalpy. However, the apparent drop in k_{obs} will be smaller than what would be calculated via an ideal diffusion model. For all but panel C), $D_{g,B} = 0.2D_{g,A} \approx D_{bulk}$.

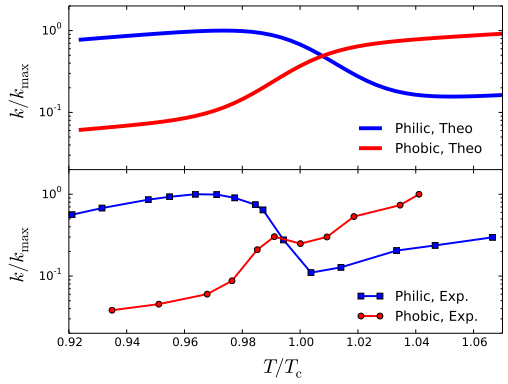

FIG. 5: Top: Normalized reaction rate as a function of temperature, in the case that $\mathcal{P}$ decreases (red curve) or increases (blue curve) upon crossing $T_{\rm LCST}$. Note that since the diffusion coefficient in the gel is always expected to drop upon polymer collapse at $T_{\rm LCST}$, an increase in $\mathcal{P}$ can be observed only if the solvation free enthalpy decreases, leading to a better interaction of the reacting molecule with the solvating gel environment, and hence to an increased concentration of reactants inside the gel. $\Delta\bar{G}_{\rm sol}$ enters exponentially in the definition of $\mathcal{P}$ (see Eq. 17), hence even a decrease of a few $k_{\rm B}T$ can offset a large reduction in diffusion coefficient. On the contrary, an increase in $\Delta\bar{G}_{\rm sol}$ can lead to an even larger reduction in the reaction rate than what would be expected by a simple reduction in the diffusion coefficient.

Evidence of the two qualitatively different behaviours we predict based on our theory can be found in recent experiments on different PNIPAM-based nanoreactor architectures,[13,15] which we show in Fig. 5. In general, one expects that for a hydrophilic molecule, the solvation free enthalpy is lower in the low-temperature, hydrophilic state of the gel compared to that in the high-temperature hydrophobic state. Hence, upon crossing $T_{\rm LCST}$ from below there will be a drop in the diffusion coefficient and an increase in the solvation free enthalpy that will exponentially reduce the reaction rate. For a hydrophobic molecule the opposite behaviour is expected. These cases are in full agreement with the experimental data.[13,15] In the first case, Carregal-Romero and coworkers looked at the reduction of hexacyanoferrate(III) ($Fe(CN)_6^{3-}$), a strongly hydrophilic molecule due to its charge, by borohydride anions using a *core-shell* nanoreactor.[13] These workers indeed found a marked drop in the reaction rate (blue squares in Fig. 5), much larger than in the expected drop in the diffusion coefficient based on Eq. (9). Instead, Wu *et al.* used yolk-shell nanoreactors to

control the reduction of 4-nitrobenzene using borohydride anions (BH_4^-). Going from below to above the T_{LCST} , gel permeability is increased in this case, inducing the observed jump in the reaction rate (red circles in Fig. 5, bottom) despite the decrease in the diffusion in the collapsed network.

IV. CONCLUSIONS

We developed a model to describe the reaction rate observed in polymer-based, stimuli-responsive catalytic nanoreactors. The theory combines a two-state thermodynamic model with the description of the reactants' diffusion which is based on Debye's theory of diffusion through a free-energy landscape. Model calculations highlight the importance of the solvation free enthalpy difference between the bulk solvent and the nanoreactor's polymeric cage. The theory predicts not only a sudden decrease in the observed rate, but also a possibility for rate enhancement, depending on the change in solvation free enthalpy at the swollen-to-collapse transition of the PNIPAM-based nanoreactors. Such rate enhancement has been observed in recent experiments[13,15] and corroborates our description. The entire treatment demonstrates that nanoreactors can be used to enhance the selectivity of catalysis by nanoparticles.

V. ACKNOWLEDGEMENTS

S. A.-U. acknowledges the Alexander von Humboldt Foundation for funding (AvH) via an Alexander von Humboldt Postdoctoral Research Fellowship. Research in the J.D. group is supported by the Deutsche Forschungsgemeinschaft (DFG), the AvH, and the ERC (European Research Council) Consolidator Grant with project number 646659 – NANOREACTOR.

Appendix: Derivation of the Debye-Smoluchowski equations

Debye's model describes the rate at which a particle, driven by gradients in chemical potential, diffuse from a bulk solution kept at constant concentration c_0 towards a sink

of radius R_{np}. Close to the sink, a fraction k_{vol} per unit time of the molecules arriving are allowed to absorb. Restated in our language, the sink is the nanoparticle inside the nanoreactor, and absorption means reacting in the proximity of the nanoparticle's surface. In order to find the number of molecules reacting per unit time, we need to find a solution for the steady state continuity equation:

$$\frac{\partial c}{\partial t} = -\nabla \cdot J(r) + k_{\text{vol}}(r)c(r) \tag{23}$$

where $J(r)$ is the flux of particles as a function of the distance from the sink (note that the problem has radial symmetry around the nanoparticle's core), and k_{vol}, the fraction of molecules reacting per unit time. Since we are considering reaction catalysed at the nanoparticle's surface, $k_{\text{vol}}(r)$ is zero everywhere except in a narrow spherical shell around the nanoparticle core, of width Δr.

We look for the steady state solution of Eq. (23), i.e.:

$$0 = -\nabla \cdot J(r) + k_{\text{vol}}(r)c(r) \tag{24}$$

which is conveniently split into two parts:

$$\begin{cases} \nabla \cdot J(r) & = k_{\text{vol}}(r)c(r); \quad r \leq R_{\text{np}} \ + \Delta r \\ \nabla \cdot J(r) & = 0; \quad r > R_{\text{np}} \ + \Delta r \end{cases} \tag{25}$$

where Δr is a very small region around the nanoparticle surface. Eq. (25) provides both a boundary condition, and a way to calculate the quantity we want, i.e. the number of particles reacting per unit time. We integrate both sides of Eq. (25) around the boundary of the reacting spherical shell, obtaining

$$\int_V \nabla \cdot J(r)dr = \int_V k_{\text{vol}}(r)c(r)dr$$
$$\int_S J(r)dA = 4\pi {R_{\text{np}}}^2 \Delta r c(R_{\text{np}})k_{vol}$$
$$4\pi {R_{\text{np}}}^2 J(R_{\text{np}}) = K_{\text{vol}} c(R_{\text{np}}) \tag{26}$$

where in the l.h.s we used the divergence theorem to transform a volume integral to a surface integral, and $\Delta V = 4\pi {R_{\text{np}}}^2 \Delta r$ is nothing but the volume of the reacting spherical shell. Hence, $\Delta V c(R_{\text{np}})$ represents the number of molecules in that volume, which multiplied by k_{vol} provides the quantity we want, the number of molecules reacting per unit time (in the last equation, we introduced the quantity K_{vol}, which will later simplify the equations). To calculate this quantity we need the concentration at the nanoparticles surface, $c(R_{\text{np}})$. To calculate its value, we first connect the flux J to the molecules concentration c, for which standard thermodynamics provides the following relation:[39]

$$J(r) = -D(r)c(r)\frac{d}{dr}\beta\mu(r) \tag{27}$$

where $D(r)$ is the (spatially dependent) diffusion coefficient and μ the chemical potential. When a molecule interacts with an external environment with a spatially dependent free enthalpy, its chemical potential is given by:

$$\beta\mu(r) = \log\left(\frac{c(r)}{c_0}\right) + \beta\Delta G_{\text{sol}}(r) \tag{28}$$

where c_0 is a reference concentration, whose value can be chosen arbitrarily. Note that by considering an ideal diffusion process, i.e. when $\Delta G_{\text{sol}}(r) = 0$, combining Eq. (27) and Eq. (28) leads to Fick's first law, i.e. $J = -D(r)\frac{d}{dr}c$, which states that the flux is simply proportional to the concentration gradient, the diffusion coefficient being the proportionality constant.

Finally, we substitute Eq. (27) into Eq. (25), then we re-write the chemical potential as a function of c using Eq. (28) and we obtain:

$$
\begin{aligned}
&\nabla \cdot \left(Dc \frac{d}{dr} \beta\mu \right) = 0 \\
&\frac{1}{r^2} \frac{d}{dr} r^2 (Dc \frac{d}{dr} \beta\mu) = 0 \\
&r^2 c \frac{d}{dr} \beta\mu = C_1 \\
&\frac{d}{dr} c + c \frac{d}{dr} \beta \Delta G_{\text{sol}} = \frac{C_1}{r^2 D}
\end{aligned} \tag{29}
$$

Eq. 29 is a nonhomogeneous ODE of first order with variable coefficients, and can be solved using the integrating factor approach[48]. In particular, one can introduce the factor $s(r) = \exp(\beta \Delta G_{\text{sol}}(r))$, which has the property $\frac{d}{dr} s = s \frac{d}{dr} \beta \Delta G_{\text{sol}}(r)$. Multiplying both sides of Eq. 29 by s we obtain

$$
\begin{aligned}
&s \frac{d}{dr} c + sc \frac{d}{dr} \beta \Delta G_{\text{sol}}(r) = \frac{C_1 s}{r^2 D} \\
&s \frac{d}{dr} c + c \frac{d}{dr} s = \frac{C_1 s}{r^2 D} \\
&\frac{d}{dr} (sc) = \frac{C_1 s}{r^2 D}
\end{aligned} \tag{30}
$$

Hence integrating both sides from R_{np} to a point r we obtain the following general solution for c:

$$
c(r) = s(r)^{-1} \left(\int_{R_{\text{np}}}^{r} \frac{C_1 s(r')}{r'^2 D(r')} dr' - c(R_{\text{np}}) s(R_{\text{np}}) \right). \tag{31}
$$

In order to determine $c(R)$ and C_1, we need to apply the boundary, Eq. (25) previously obtained, as well as imposing that in the bulk far from the nanoparticle the concentration must equal the bulk concentration c_0, or in mathematical form $\lim_{r \to \infty} c(r) = c_0$. We obtain in this way:

$$c(r) = \frac{I(r)K_{\rm vol}c_0 + 4\pi c_0 \exp[\beta\Delta G_{\rm sol}\left(R_{\rm np}\right)]}{\exp[\beta\Delta G_{\rm sol}\left(r\right)]\left(I(\infty)K_{\rm vol} + 4\pi \exp[\beta\Delta G_{\rm sol}\left(R_{\rm np}\right)]\right)} \tag{32}$$

where we introduced the function $I(r) = \int_{R_{\rm np}}^{r} \frac{exp[\beta\Delta \bar{G}_{\rm sol}\ (r')]}{D(r')r'^2}dr'$. One can check that Eq. 32 correctly reproduces some interesting limit. For example, if $K_{\rm vol} = 0$ there is no reaction taking place and the equilibrium concentration must be attained, which must comply with Boltzmann's form, and one indeed obtains $c(r) = c_0 \exp[-\beta\Delta G_{\rm sol}\left(r\right)]$. Moreover, the same result is obtained if the system has an infinite diffusion coefficient $D(r)$ (hence $I(r) = 0$), in which case it must also always relax to instantaneously to equilibrium.

Given Eq. (32), we can finally calculate the number of particles reacting per unit time, given by $k_{\rm t} = K_{\rm vol}c(R)$, for which we obtain:

$$k_{\rm t} = \frac{4K_{\rm vol}\pi c_0}{I(\infty)K_{\rm vol} + 4\pi \exp[\beta\Delta G_{\rm sol}\left(R_{\rm np}\right)]} \tag{33}$$

It is quite instructive to rewrite $k_{\rm t}$ in the following form:

$$\begin{aligned} k_{\rm t}^{-1} &= [K_{\rm vol}c_0 \exp[-\beta\Delta G_{\rm sol}\left(R_{\rm np}\right)]]^{-1} + k_{\rm D}^{-1} \\ &= k_{\rm R}^{-1} + k_{\rm D}^{-1} \end{aligned} \tag{34}$$

where

$$k_{\rm D} = \frac{4\pi c_0}{I_\infty}. \tag{35}$$

Eqs. (32), (33), (34) and (35) constitute Debye's theory in its most general form.
It is interesting to see what is the interpretation of Eq. 34: if the diffusion coefficient was infinitely fast, the concentration at each point in space would not be influenced by the presence of the sink and would correspond to the equilibrium concentration. In fact, from Eq. 32 we obtain $c(r) = c_0 \exp(-\beta \Delta G_{\mathrm{sol}}(r)) = c^{eq}(r)$. In this case, the number of particles reacting per unit time at the sink would be simply $k_{\mathrm{R}} = K_{\mathrm{vol}} c_{eq}(r)$. Note that quite often the factor $\exp[-\beta \Delta G_{\mathrm{sol}}(R_{\mathrm{np}})]$ is forgotten in the literature. However, for both mathematical and physical consistency this factor must be introduced if the effect of energy gradients have to be taken into account. Hence not only k_{D} but also k_R is influenced by the solvation free enthalpy. Also, it is evident that k_{D} is the reaction rate which would be obtained if the surface reaction rate k_{R} was infinitely fast, so that any molecule hitting the surface would immediately react (formally $c(R) = 0, \quad K_{vol} = \infty$). In this case, k_{D} is exactly the reaction rate obtained for a purely diffusion limited process.

---

* Electronic address: Joachim.dzubiella@helmholtz-berlin.de

[1] Astruc, D. *Nanoparticles and Catalysis*; 2008; pp 1–640.

[2] Hutchings, G. J.; Edwards, J. K. *Frontiers of Nanoscience* **2012**, *3*, 249–293.

[3] Haruta, M. *Chemical Record* **2003**, *3*, 75–87.

[4] Hutchings, G. J.; Haruta, M. *Applied Catalysis A: General*; 2005; Vol. 291; pp 2–5.

[5] Thompson, D. T. *Nano Today* **2007**, *2*, 40–43.

[6] Yurdakal, S.; Augugliaro, V.; Sanz, J.; Soria, J.; Sobrados, I.; Torralvo, M. J. *Journal of Catalysis* **2014**, *309*, 97–104.

[7] Graciani, J.; Sanz, J. F. Designing a new generation of catalysts: Water gas shift reaction example. 2014.

[8] Crooks, R. M.; Zhao, M.; Sun, L.; Chechik, V.; Yeung, L. K. *Accounts of Chemical Research* **2001**, *34*, 181–190.

[9] Ballauff, M. Spherical polyelectrolyte brushes. 2007.

[10] Lu, Y.; Mei, Y.; Drechsler, M.; Ballauff, M. *Angewandte Chemie - International Edition* **2006**, *45*, 813–816.

[11] Lu, Y.; Ballauff, M. *Progress in Polymer Science (Oxford)* **2011**, *36*, 767–792.

[12] Contreras-Cáceres, R.; Sánchez-Iglesias, A.; Karg, M.; Pastoriza-Santos, I.; Pérez-Juste, J.; Pacifico, J.; Hellweg, T.; Fernández-Barbero, A.; Liz-Marzán, L. M. *Advanced Materials* **2008**, *20*, 1666–1670.

[13] Carregal–Romero, S. and Buurma, N. J. and Perez–Juste, J. and Liz–Marzan, L. M. and Hervés, P., *Chem. Mater.* **2010**, *22*, 3051–3059.

[14] Lu, Y.; Proch, S.; Schrinner, M.; Drechsler, M.; Kempe, R.; Ballauff, M. *J. Mater. Chem.* **2009**, *19*, 3955–3961.

[15] Wu, S.; Dzubiella, J.; Kaiser, J.; Drechsler, M.; Guo, X.; Ballauff, M.; Lu, Y. *Angew. Chem. Int. Ed.* **2012**, *51*, 2229 2233.

[16] Horecha, M.; Kaul, E.; Horechyy, A.; Stamm, M. *Journal of Materials Chemistry A* **2014**, *2*, 7431.

[17] Chen, J.; Xiao, P.; Gu, J.; Han, D.; Zhang, J.; Sun, A.; Wang, W.; Chen, T. *Chemical communications (Cambridge, England)* **2014**, *50*, 1212–4.

[18] Pradhan, N.; Pal, A.; Pal, T. *Colloids and Surfaces A: Physicochemical and Engineering Aspects* **2002**, *196*, 247–257.

[19] Esumi, K.; Miyamoto, K.; Yoshimura, T. *Journal of Colloid and Interface Science* **2002**, *254*, 402–405.

[20] Mei, Y.; Sharma, G.; Lu, Y.; Ballauff, M.; Drechsler, M.; Irrgang, T.; Kempe, R. *Langmuir* **2005**, *21*, 12229–12234.

[21] Schrinner, M.; Ballauff, M.; Talmon, Y.; Kauffmann, Y.; Thun, J.; Möller, M.; Breu, J. *Science (New York, N.Y.)* **2009**, *323*, 617–620.

[22] Wunder, S.; Polzer, F.; Lu, Y.; Mei, Y.; Ballauff, M. *Journal of Physical Chemistry C* **2010**, *114*, 8814–8820.

[23] Wunder, S.; Lu, Y.; Albrecht, M.; Ballauff, M. *ACS Catalysis* **2011**, *1*, 908–916.

[24] Kaiser, J.; Leppert, L.; Welz, H.; Polzer, F.; Wunder, S.; Wanderka, N.; Albrecht, M.; Lunkenbein, T.; Breu, J.; Kümmel, S.; Lu, Y.; Ballauff, M. *Physical Chemistry Chemical Physics* **2012**, *14*, 6487.

[25] Gu, S.; Wunder, S.; Lu, Y.; Ballauff, M.; Fenger, R.; Rademann, K.; Jaquet, B.; Zaccone, A. *The Journal of Physical Chemistry C* **2014**, *118*, 18618–18625.

[26] Xia, Y.; Shi, Z.; Lu, Y. *Polymer* **2010**, *51*, 1328–1335.

[27] Zeng, J.; Zhang, Q.; Chen, J.; Xia, Y. *Nano Letters* **2010**, *10*, 30–35.

[28] Antonels, N. C.; Meijboom, R. **2013**,

[29] Nemanashi, M.; Meijboom, R. *Journal of Colloid and Interface Science* **2013**, *389*, 260–267.

[30] Zhang, H.-X.; Liu, M.; Bu, X.; Zhang, J. *Scientific reports* **2014**, *4*, 3923.

[31] Chi, Y.; Tu, J.; Wang, M.; Li, X.; Zhao, Z. *Journal of Colloid and Interface Science* **2014**, *423*, 54–59.

[32] Li, A.; Luo, Q.; Park, S. J.; Cooks, R. G. *Angewandte Chemie - International Edition* **2014**, *53*, 3147–3150.

[33] Shah, D.; Kaur, H. *Journal of Molecular Catalysis A: Chemical* **2014**, *381*, 70–76.

[34] Hervés, P.; Pérez-Lorenzo, M.; Liz-Marzán, L. M.; Dzubiella, J.; Lu, Y.; Ballauff, M. *Chemical Society Reviews* **2012**, *41*, 5577.

[35] Debye, P. *Trans. Electrochem. Soc.* **1942**, *92*, 265–272.

[36] Smoluchowsky, M. *Z. Physik Chem.* **1917**, *92*, 129.

[37] Zaccone, A.; Crassous, J. J.; Béri, B.; Ballauff, M. *Phys. Rev. Lett.* **2011**, *107*, 168303.

[38] Heyda, J.; Muzdalo, A.; Dzubiella, J. *Macromolecules* **2013**, *46*, 1231–1238.

[39] Angioletti-Uberti, S.; Ballauff, M.; Dzubiella, J. *Soft Matter* **2014**, *10*, 7932–7945.

[40] Amsden, B. *Macromolecules* **1998**, *31*, 8382–8395.

[41] Masaro, L.; Zhu, X. *Progress in polymer science* **1999**, *24*, 731–775.

[42] Calef, D.; Deutch, J. *Ann. Rev. Phys. Chem.* **1983**, *34*, 493–524.

[43] Berg, O.; von Hippel, P. *Ann. Rev. Biophys. Biophys. Chem.* **1985**, *14*, 131–160.

[44] Jackson, M. B. *Molecular and cellular biophysics*; Cambridge University Press, 2006.

[45] Herves, P.; Pérez-Lorenzo, M.; Liz-Marzán, L. M.; Dzubiella, J.; Lu, Y.; Ballauff, M. *Chemical Society Reviews* **2012**, *41*, 5577–5587.

[46] Hänggi, P.; Talkner, P.; Borkovec, M. *Reviews of Modern Physics* **1990**, *62*, 251.

[47] Gammaitoni, L.; Hänggi, P.; Jung, P.; Marchesoni, F. *Reviews of Modern Physics* **1998**, *70*, 223.

[48] Morse, P. M.; Feshbach, H. *"Methods of Theoretical Physics, Part I."*; New York: McGraw-Hill, 1953; pp 526–529.